

Theory of the Auger decay in one-dimensional metals: Tomonaga-Luttinger model

E. Perfetto

Dipartimento di Fisica, Università di Roma Tor Vergata, Via della Ricerca Scientifica 1, 00133 Roma, Italy

(Received 12 December 2007; revised manuscript received 14 January 2008; published 4 March 2008)

We present a dynamical theory of the Auger decay in one-dimensional metals described by the Tomonaga-Luttinger model. An analytic expression of the Auger current is derived in the framework of the one-step approach, where the finite lifetime of the initial core hole and the core-valence interaction are taken into account. This allows us to capture typical dynamical features like the *shake-down* effect, in which the Auger spectrum shows a nonvanishing weight above the two-step high-energy threshold. The obtained results give also a hint to understand the sizable suppression of Auger spectral weight close to the Fermi energy recently observed in carbon nanotubes with respect to graphite.

DOI: [10.1103/PhysRevB.77.115401](https://doi.org/10.1103/PhysRevB.77.115401)

PACS number(s): 71.10.Pm, 32.80.Hd, 79.20.Fv

I. INTRODUCTION

The dynamics of the core-valence-valence (CVV) Auger transitions in strongly correlated solids has been extensively studied during the past three decades.¹ However, despite the great interest devoted to this problem, several aspects are still not well understood. The theoretical calculation of the Auger spectrum of correlated solids is a challenging task because, besides the intrinsic difficulty of dealing with a many-body interacting system, the creation of the core-hole and the Auger process itself are, in principle, coherent events, involving virtual Auger transitions and incomplete relaxation phenomena.² The complete formulation of the theory describing the Auger decays has been provided in 1980 by Gunnarsson and Schönhammer (GS).² In the framework of the so-called one-step approach, they derived a general formula for the Auger current by treating the decay of the initial core hole to all orders. Unfortunately, such formulation cannot be cast in terms of Green's functions and is hard to implement for practical purposes. A significant progress can be done within the two-step approximation, where the photoemission and the Auger decay are considered as independent events. In this framework, Cini³ and Sawatzky⁴ (CS) proposed a simple and elegant theory able to provide a quantitative understanding of the experimental Auger spectra of transition metals with (almost) closed valence bands. An advantage of such theory is that it also provides a practical scheme to estimate the value of the screened interaction from the experimental spectra.⁵⁻⁷ This is particularly useful to support LDA+*U* calculations.⁸ In the case of open-band systems, the CS approach breaks down and no reliable theory is currently available. Very recently, Seibold *et al.*⁹ presented a theory of the dynamical two-particle response function in the two-dimensional (2D) Hubbard model based on the time-dependent Gutzwiller approximation. Although important effects are not treated there (e.g., the finite lifetime of the core hole and the interaction of the core hole with the valence electrons), the theory provides a different tool to attack the calculation of the Auger spectrum in correlated open-band systems.

In this paper, we develop a dynamical theory of the CVV Auger transitions in an ideal one-dimensional (1D) metal. In the CVV Auger decay, two holes are left in the valence band

after the x-ray photoemission of a deep core hole. Here, assume that the valence electrons form the so-called Luttinger liquid (LL), described by the Tomonaga-Luttinger model. We also allow for the interaction between the core hole and the valence electrons, and introduce a term responsible for the Auger transition, which destroys the core hole and creates the Auger electron together with the two valence holes (and vice versa). The corresponding Auger current is calculated analytically by using the bosonization and equations of motion methods.

The paper is organized as follows. In Sec. II, we describe in detail the model Hamiltonian used in the present work. In Sec. III, we derive a closed analytic expression for the Auger current in the framework of the one-step approach. In Sec. IV, we discuss the relevant features emerging from the obtained formula. In particular, we show that the theory exposed here is able to capture some striking features recently observed in the Auger spectra of carbon nanotubes. Finally, a brief summary and the main conclusions are drawn in Sec. V.

II. MODEL

The LL is the prototype of interacting electrons confined in one spatial dimension, characterized by striking phenomena such as the so-called spin-charge separation and the power-law dependence of observables in proximity of the Fermi energy.¹⁰⁻¹⁵ In Tomonaga-Luttinger Hamiltonian, the electrons have a linear dispersion relation around positive (right) and negative (left) Fermi points and the electron-electron (e-e) interactions act only between right and left electron densities. The model is exactly solvable by means of the bosonization technique, which allows us to write the electron Hamiltonian in terms of boson operator¹⁶ *b*'s:

$$\begin{aligned}
 H_{\text{Lutt}} = & \sum_{q \neq 0, \sigma} \frac{v_F}{2} |q| [b_{\sigma}^{\dagger}(q) b_{\sigma}(q) + b_{\sigma}(q) b_{\sigma}^{\dagger}(q)] \\
 & + \sum_{q \neq 0, \sigma} \frac{g_4}{4\pi} |q| [b_{\sigma}^{\dagger}(q) b_{\sigma}(q) + b_{\sigma}(q) b_{\sigma}^{\dagger}(q)] \\
 & + b_{\sigma}^{\dagger}(q) b_{-\sigma}(q) + b_{\sigma}(q) b_{-\sigma}^{\dagger}(q)] \\
 & - \sum_{q \neq 0, \sigma} \frac{g_2}{4\pi} |q| [b_{\sigma}^{\dagger}(q) b_{\sigma}^{\dagger}(-q) + b_{\sigma}(q) b_{\sigma}(-q)]
 \end{aligned}$$

$$+ b_{\sigma}^{\dagger}(q)b_{-\sigma}^{\dagger}(-q) + b_{\sigma}(q)b_{-\sigma}(-q)], \quad (1)$$

where $\sigma = \uparrow, \downarrow$ is the spin index, $[b_{\sigma}(q), b_{\sigma'}^{\dagger}(q')] = \delta_{\sigma, \sigma'} \delta_{q, q'}$, v_F is the Fermi velocity, g_4 is the interaction parameter between right-right (positive q) and left-left (negative q) electron densities, while g_2 is the interaction parameter between left and right densities.

The key point of the bosonization is that it is possible to express the fermion fields in terms of boson fields. Here, it is useful to introduce a chirality index $\nu = R, L$ to distinguish between right and left electron modes. For instance, the $\nu = R$ fermion field is given by

$$\psi_{\sigma, R}(x) = \frac{\eta_{R, \sigma}}{(2\pi\alpha)^{1/2}} e^{i\Phi_{\sigma, R}(x)}, \quad (2)$$

where $\eta_{R, \sigma}$ is an anticommuting Klein factor and

$$\begin{aligned} \Phi_{\sigma, R}(x) = & \sum_{q>0} \left(\frac{2\pi}{qL} \right)^{1/2} e^{-\alpha q/2} [b_{\sigma}^{\dagger}(q)e^{-iqx} + b_{\sigma}(q)e^{iqx}] + \varphi_{0, R} \\ & + \frac{2\pi x N_R}{L}, \end{aligned} \quad (3)$$

where N_R is the total number of right electrons, $[\varphi_{0, R}, N_R] = i$, and L is the length of the system. α is a short-distance cutoff that must be introduced in order to have converging integrals.¹⁷ In principle, the bosonization provides exact results in the limit $\alpha \rightarrow 0$; however, for practical purposes, it is useful to take a nonzero (small) α which introduces a finite effective bandwidth $\gamma = v_F/\alpha$ in the system. By doing this, we have to bear in mind that such procedure gives an accurate physical description only in the low-energy part of the spectrum.¹⁸

The coupling of valence electrons to the core hole is given by^{2,19,20}

$$H_{\lambda} = \sqrt{\frac{2\pi}{L}} \sum_{q \neq 0} \sum_{\sigma} \lambda(q) [b_{\sigma}^{\dagger}(q) + b_{\sigma}(q)] (1 - n_c), \quad (4)$$

where $\lambda(q)$ is the core-valence coupling constant, L is the volume of the system, $c_c^{(\dagger)}$ is the annihilation (creation) operator of the core electron, whose occupancy and energy are $n_c = c_c^{\dagger} c_c$ and ε_c , respectively. In the following, we will take $\lambda(q) \equiv \lambda$.

The term responsible for the Auger decay is more conveniently expressed in the fermionic representation and reads

$$H_A = c_p^{\dagger} c_c^{\dagger} A + \text{H.c.}, \quad A = V \psi_{\uparrow}(0) \psi_{\downarrow}(0), \quad (5)$$

where $c_p^{(\dagger)}$ destroys (creates) the Auger electron and

$$\psi_{\sigma} = \psi_{\sigma, R} + \psi_{\sigma, L}. \quad (6)$$

V is the so-called Auger matrix element, which, here, is taken as a constant. Here, we are assuming for simplicity that the CVV decay leaves the two final holes in the origin of the system in a singlet configuration. This reflects the local nature of the Auger process; however, such assumption is not essential and could be relaxed.

As long as the interactions do not depend on spin, H_{Lutt} can be diagonalized by introducing charge and spin boson

operators: $b_{c, s}^{(\dagger)}(q) = [b_{\uparrow}^{(\dagger)}(q) \pm b_{\downarrow}^{(\dagger)}(q)]/\sqrt{2}$, and performing a Bogoliubov transformation in the charge sector: $\tilde{b}_c(q) = \cosh \varphi b_c(q) + \sinh \varphi b_c^{\dagger}(-q)$ and $\tilde{b}_c^{\dagger}(q) = \sinh \varphi b_c(-q) + \cosh \varphi b_c^{\dagger}(q)$, with $\tanh 2\varphi = (g_2/\pi)/[v_F + (g_4/\pi)]$ and renormalized velocity $v = \{[v_F + (g_4/\pi)]^2 - (g_2/\pi)^2\}^{1/2}$. In the next section, we use the bosonization scheme sketched above to compute the Auger spectrum of a 1D metal described within the Luttinger liquid theory.

III. CALCULATION OF THE AUGER SPECTRUM

The one-step formulation of the Auger processes has been provided by GS,^{2,21} who showed that the Auger current is given by the following correlator:^{2,22}

$$j(\omega) = \frac{\pi\alpha^2}{2} \int_0^{\infty} dt \int_0^{\infty} dt' e^{i\omega(t-t')} f(t, t'), \quad (7)$$

where the factor $\pi\alpha^2/2$ is chosen in order to have a normalized spectrum and

$$f(t, t') = \langle g | c_c^{\dagger} e^{i(H[0] + i\hat{\Gamma})t'} c_c A^{\dagger} e^{iH[1](t-t')} A c_c^{\dagger} e^{-i(H[0] - i\hat{\Gamma})t} c_c | g \rangle. \quad (8)$$

In the above expression, $|g\rangle$ is the ground state before the x-ray photoemission, $H[0, 1]$ is the Hamiltonian of the system $H = H_{\text{Lutt}} + \varepsilon_c(1 - n_c) + H_{\lambda}$, with $n_c = 0$ and 1, respectively, and $\hat{\Gamma}$ is an effective optical potential describing virtual Auger transitions and relaxation processes.² In order to proceed, we make the following approximation:

$$\begin{aligned} f(t, t') & \approx \langle \tilde{g} | e^{i\tilde{H}[0]t'} A^{\dagger} e^{iH[1](t-t')} A e^{-i\tilde{H}[0]t} | \tilde{g} \rangle e^{-i\varepsilon_c(t-t')} e^{-\Gamma(t+t')} \\ & \equiv C(t, t') e^{-i\varepsilon_c(t-t')} e^{-\Gamma(t+t')}, \end{aligned} \quad (9)$$

where the second line of the above equation is the core-hole Green's function with lifetime $1/\Gamma$, which is a c -number. $|\tilde{g}\rangle$ denotes the ground state of H_{Lutt} (whose elementary excitations are created by \tilde{b}_c^{\dagger} and b_s^{\dagger}), describing the valence band in the initial state, and $\tilde{H}[0] \equiv H[0] - \varepsilon_c$. As noticed by GS,² the strength of the effective optical potential is proportional to the square of the Auger matrix element, and hence we can replace V^2 by Γ . $C(t, t')$ can be calculated exactly by using the bosonization formulas in Eqs. (2) and (3) and the equations of motion method. After some algebra, one gets a compact expression by introducing new variables $\tau = t - t'$ and $T = (t + t')/2$:

$$C(\tau, T) = \frac{\Gamma}{2\pi} \left[\frac{\alpha^g e^{h(\tau, T)}}{(-i\tau v + \alpha)^g} + \frac{\alpha^{l+1} e^{k(\tau, T)}}{(-i\tau v + \alpha)^l (-i\tau v_F + \alpha)} \right], \quad (10)$$

where we have defined $g = 2(\cosh^2 \varphi + \sinh^2 \varphi)$ and $l = (\cosh \varphi + \sinh \varphi)^2$. The complex functions $h(\tau, T)$ and $k(\tau, T)$ are reported in the Appendix. Finally, the Auger current reads

$$j(\omega - \varepsilon_c) = \int_{-\infty}^{\infty} d\tau \int_0^{\infty} dT e^{i\omega\tau} e^{-2\Gamma T} C(\tau, T), \quad (11)$$

where we refer the kinetic energy of the Auger electron ω with respect to the core-level energy ε_c . Equations (10) and (11) constitute the main finding of the present work. In the next section, we discuss the most relevant features emerging from Eqs. (10) and (11), which give a hint to understand the physics of the Auger transitions in 1D systems.

IV. DISCUSSION

We first observe that despite the LL nature of the valence electrons, the correlator $C(\tau, T)$ does *not* obey a power law, which is spoiled by the interaction λ between the valence electrons and the core hole. It is also interesting to study the relationship of our solution with the two-step approach. This is done in the limit $\Gamma \rightarrow 0$. As discussed by GS, if such limit exists, one should recover the well-known two-step solution since the Auger transition happens after the complete relaxation of the initial state. Such limit is carried out by observing that

$$\lim_{\Gamma \rightarrow 0} 2\Gamma \int_0^{\infty} dT e^{-2\Gamma T} e^{z(\tau, T)} = \lim_{T \rightarrow \infty} e^{z(\tau, T)}, \quad (12)$$

with $z=h$ and k . We note that for any finite $\tilde{\lambda}$, the limit on the right hand side does not exist, because for large T , we have $h(\tau, T) \sim k(\tau, T) \sim (\tilde{\lambda}/v)^2 i v \tau \ln(vT/a)$. This is a remarkable result, showing that the two-step approach is *not* justified if the valence band, is described by the LL. On the other hand, if we set $\tilde{\lambda}=0$, the one-step and two-step solutions do coincide because the two-step spectrum is obtained from the two-particle Green's function describing the valence electrons (holes) in the ground state of H_{Lutt} . The two-step approach is often employed in typical Auger calculations and, therefore, it is instructive to compare it with our one-step solution. The two-step Auger current is readily obtained by setting $\tilde{\lambda}=0$ and results in

$$j_{\text{two-step}}(\omega - \varepsilon_c) = \int_{-\infty}^{\infty} d\tau \frac{e^{i\omega\tau}}{4\pi} \left[\frac{\alpha^g}{(-i\tau v + \alpha)^g} + \frac{\alpha^{l+1}}{(-i\tau v + \alpha)^l (-i\tau v_F + \alpha)} \right], \quad (13)$$

which recovers the characteristic power-law suppression at $\omega \approx 0$. The comparison between the Auger spectra calculated with $j(\omega - \varepsilon_c)$ and $j_{\text{two-step}}(\omega - \varepsilon_c)$ is shown in Fig. 1. As discussed above, it is seen that j does not approach $j_{\text{two-step}}$ for small Γ (compared to γ). In particular, we note that for $\Gamma \rightarrow 0$, the center of gravity ε_g of j (stars and circles) is shifted toward lower kinetic energies with respect to the center of gravity of $j_{\text{two-step}}$ (triangles) with a logarithmic dependence $\varepsilon_g \propto \tilde{\lambda}^2 \ln(\Gamma a/v)$.

Another interesting case is obtained in the limit $\Gamma \rightarrow \infty$, that is, for very short core-hole lifetime. In this case, $2\Gamma e^{-2\Gamma T}$ produces a Dirac delta in the T integration:

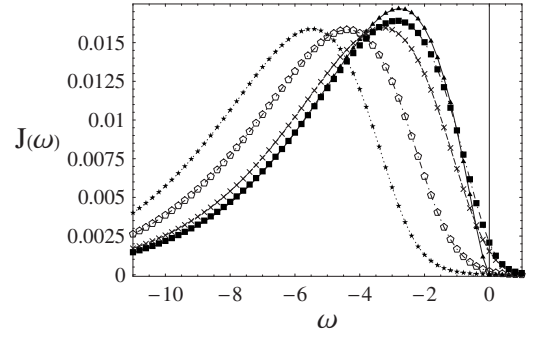


FIG. 1. Auger current $j(\omega - \varepsilon_c)$ calculated numerically from Eq. (11) for different values of the core-hole lifetime and core-valence interaction: $\Gamma/\gamma=0.001$ (stars), $\Gamma/\gamma=0.01$ (circles), $\Gamma/\gamma=0.1$ (crosses), and $\Gamma/\gamma=\infty$ (boxes). Here, we have taken $g_4=g_2=4$, $\alpha=0.1$, $v_F=1$, $a=1$, and $\lambda=4$ except in triangle curve, where $\lambda=0$. ω is expressed in units of γ . The vertical line denotes the two-step high-energy threshold ε_c , set equal to zero in the present figure.

$$\lim_{\Gamma \rightarrow \infty} 2\Gamma \int_0^{\infty} dT e^{-2\Gamma T} e^{z(\tau, T)} = e^{z(\tau, 0)}, \quad (14)$$

with $z=h$ and k . In this limit, the Auger transition occurs when the initial state is still excited, since $e^{-i\tilde{H}[0]t}|\tilde{g}\rangle$ is not an eigenstate of $H[1]$. As a consequence, the excitations created on emission of the initial core electron transfer their energy to the Auger electron, which then has a kinetic energy exceeding the high-energy threshold ε_c in the two-step model [see Eq. (13) and Fig. 1 (boxes)]. This phenomenon, known as shake down, is a typical example of qualitative departures from the predictions of the two-step model.

Finally, we show that our theory provides an explanation of the sizable suppression of CVV Auger spectral weight close to the Fermi energy observed in carbon nanotubes with respect to graphite.^{23,24} This is a striking trend, since the structure of the one-particle density of states (1PDOS) of the two carbon structures would predict the opposite behavior. In fact, while in metallic nanotubes the 1PDOS at the Fermi energy is *finite* due to the 1D linear dispersion, in graphite it is *vanishing*, due to the 2D conical dispersion. Therefore, we expect that correlation effects have to be invoked in order to revert the one-particle scenario.

Metallic carbon nanotubes are believed to be rather good (although approximate) realizations of LL²⁵⁻²⁷ since in normal conditions the main correlation effects come from the long-range part of the Coulomb repulsion. In nanotubes with radius R , the backscattering interactions with large momentum transfer suffer a $1/R$ suppression.^{28,29} Therefore, we believe that typical metallic (10,10) nanotubes are well described by the present theory. Concerning graphite, we use the CS approach, which is known to give the Auger spectrum in excellent agreement with experimental one.^{24,30} In order to employ the CS approach, we must compute the two-particle valence Green's function within the bare ladder approximation.³⁴ This is accomplished starting from the non-interacting valence 1PDOS

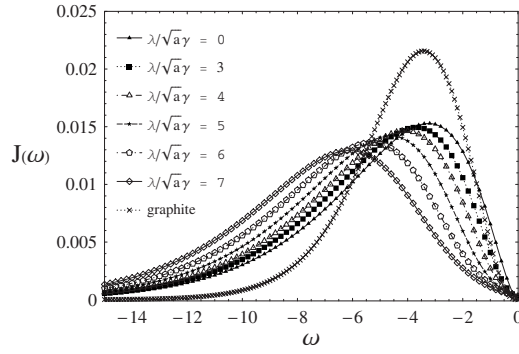


FIG. 2. Comparison between the calculated Auger current for graphite $j_{CS}^{2D}(\omega - \varepsilon_c)$ (crosses curve) and (10,10) single-walled nanotubes $j(\omega - \varepsilon_c)$ according to Eq. (11) for different values of the core-valence interaction. ω is expressed in units of γ , and ε_c is set equal to zero.

$$\rho_0^{2D}(\omega) = \gamma^{-2} \theta(-\omega) |\omega| e^{-|\omega|/\gamma}, \quad (15)$$

which is obtained by imposing the 2D linear spectrum $\varepsilon(k_x, k_y) = v_F(k_x^2 + k_y^2)^{1/2}$ and the momentum cutoff $1/\alpha$. We note in passing that ρ_0^{2D} vanishes linearly at $\omega=0$, as it should. The corresponding noninteracting two-particle Green's function G_0^{2D} is obtained by self-folding ρ_0^{2D} and by Hilbert transforming:

$$G_0^{2D}(\omega) = (1/6\gamma) [2 - (\omega/\gamma) + 2(\omega/\gamma)^2 - (\omega/\gamma)^3 e^{\omega/\gamma} \Gamma(0, \omega/\gamma)], \quad (16)$$

where $\Gamma(x, y)$ is the incomplete gamma function. Thus, the Auger spectrum of graphite according to CS theory is³¹

$$j_{CS}^{2D}(\omega - \varepsilon_c) = -\frac{1}{\pi} \text{Im} \left[\frac{G_0^{2D}(-\omega + i0^+)}{1 - U G_0^{2D}(-\omega + i0^+)} \right], \quad (17)$$

where U is the short-range screened repulsion felt by the two valence holes in the final state. It is worthy to recall that our model is suitable to represent the π electrons of nanotubes and graphite, which are the ones involved in proximity of the Fermi level (placed at $\omega=0$). Therefore, only the low-energy portion of the experimental Auger spectra can be addressed within the present framework, while the high-energy spectral region, corresponding to deep σ_p and σ_s states, cannot be described here. A complete analysis including the missing σ_p and σ_s states can be found in Ref. 24. However, in that paper, the suppression of the Auger spectrum of nanotubes close to the Fermi energy was reproduced by including some phenomenological form factors which have been fitted with the experimental data. Conversely, in the present work, the problem is treated starting from a fully microscopic theory with no adjustable parameter.

In order to compare with the experiment, we use the following realistic values for graphite and (10,10) metallic nanotubes: $v_F \approx 10^6$ m/s, α such that $\gamma = v_F/\alpha \approx 10$ eV, $\Gamma \approx 0.2$ eV (Ref. 32) (i.e., $\Gamma/\gamma = 0.02$), $g_4 = g_2 \approx 2e^2 \ln(L/R)/\kappa \approx 5v_F$,^{33,34} $a \approx 1$ Å, $U \approx 2$ eV,^{24,6} and leaving the adimensional ratio $\lambda/\sqrt{a}\gamma$ as free parameter. In Fig. 2, we see that the inclusion of e-e correlations in carbon

nanotubes according to the LL theory within the two-step approach (black solid line) is not enough to reproduce the suppression of j vs j_{CS}^{2D} close to $\omega \sim 0$. On the other hand, the full one-step theory with finite $\lambda/\sqrt{a}\gamma \geq \gamma$ provides results in qualitative agreement with the experimental trend.³⁵ This is a quite reasonable finding, considering that the core-valence repulsion is larger than (but of the same order of) the valence-valence repulsion.

V. SUMMARY AND CONCLUSIONS

Traditional photoemission and inverse photoemission experiments which probe one-particle dynamical responses provide a well-established tool for the understanding of strongly correlated 1D systems. A great amount of theoretical work devoted to this problem has been published in the past, enlightening the role of the LL concept to explain several features.¹⁰⁻¹⁵

Surprisingly, the study of the 1D Auger transitions, which are related to the two-particle dynamics, has been only poorly addressed. On the other hand, the Auger spectroscopy is a powerful experimental technique which permits the characterization of the correlations in solids and, therefore, is of crucial importance in the study of strongly correlated systems.

In the present work, we have developed a dynamical theory of the Auger processes in 1D metals described within the LL theory. Our theory includes the finite core-hole lifetime and the valence-valence and the core-valence interactions as well. A typical one-step feature is observed in the limit of small core-hole lifetime, in which the valence electrons cannot relax before the Auger transition, and the shake-down phenomenon occurs. Remarkably, it is shown that the two-step approximation is not valid for any finite core-valence interaction, which also spoils the low-energy power-law behavior typically expected in the LL. Only for vanishing core-valence interaction, the power-law is recovered. Finally, we have shown that our one-step theory is able to reproduce the low-energy suppression of Auger spectral weight observed in carbon nanotubes with respect to graphite.

ACKNOWLEDGMENT

The author kindly acknowledges M. Cini for helpful discussions.

APPENDIX: FUNCTIONS $h(\tau, T)$ AND $k(\tau, T)$

The final expression for $C(t, t')$ in Eq. (10) has been obtained by employing the bosonization formulas in Eqs. (2) and (3) and the equations of motion method. In order to perform the sum over q , we used $q = 2\pi n/L$ and took the large- L limit. When doing this, it is useful to set $L = aN$, where N is the number of sites of the 1D system and a is the lattice constant, and send $N \rightarrow \infty$. The functions $h(\tau, T)$ and $k(\tau, T)$ obtained in this way read

$$\begin{aligned}
h(\tau, T) = & -\frac{\tilde{\lambda}}{v} 2i\sqrt{\pi}(\cosh \varphi - \sinh \varphi) \left[\sqrt{3\alpha + 2iv\left(T + \frac{\tau}{2}\right)} + \sqrt{3\alpha - 2iv\left(T + \frac{\tau}{2}\right)} - \sqrt{3\alpha + 2iv\left(T - \frac{\tau}{2}\right)} - \sqrt{3\alpha - 2iv\left(T - \frac{\tau}{2}\right)} \right] \\
& + \left(\frac{\tilde{\lambda}}{v}\right)^2 \left\{ -4\alpha \ln\left(\frac{2\alpha}{a}\right) + 2(2\alpha - iv\tau) \ln\left(\frac{2\alpha - iv\tau}{a}\right) + \left[\alpha - iv\left(T - \frac{\tau}{2}\right)\right] \ln\left[\frac{\alpha - iv\left(T - \frac{\tau}{2}\right)}{a}\right] \right. \\
& - \left[\alpha + iv\left(T - \frac{\tau}{2}\right)\right] \ln\left[\frac{\alpha + iv\left(T - \frac{\tau}{2}\right)}{a}\right] - \left[\alpha - iv\left(T + \frac{\tau}{2}\right)\right] \ln\left[\frac{\alpha - iv\left(T + \frac{\tau}{2}\right)}{a}\right] \\
& \left. + \left[\alpha + iv\left(T + \frac{\tau}{2}\right)\right] \ln\left[\frac{\alpha + iv\left(T + \frac{\tau}{2}\right)}{a}\right] \right\}
\end{aligned} \tag{A1}$$

and

$$\begin{aligned}
k(\tau, T) = & \left(\frac{\tilde{\lambda}}{v}\right)^2 \left\{ -4\alpha \ln\left(\frac{2\alpha}{a}\right) + 2(2\alpha - iv\tau) \ln\left(\frac{2\alpha - iv\tau}{a}\right) + \left[\alpha - iv\left(T - \frac{\tau}{2}\right)\right] \ln\left[\frac{\alpha - iv\left(T - \frac{\tau}{2}\right)}{a}\right] \right. \\
& - \left[\alpha + iv\left(T - \frac{\tau}{2}\right)\right] \ln\left[\frac{\alpha + iv\left(T - \frac{\tau}{2}\right)}{a}\right] - \left[\alpha - iv\left(T + \frac{\tau}{2}\right)\right] \ln\left[\frac{\alpha - iv\left(T + \frac{\tau}{2}\right)}{a}\right] \\
& \left. + \left[\alpha + iv\left(T + \frac{\tau}{2}\right)\right] \ln\left[\frac{\alpha + iv\left(T + \frac{\tau}{2}\right)}{a}\right] \right\},
\end{aligned} \tag{A2}$$

with $\tilde{\lambda} = \lambda\sqrt{2}(\cosh \varphi - \sinh \varphi)$.

¹For a review, see, e.g., C. Verdozzi, M. Cini, and A. Marini, J. Electron Spectrosc. Relat. Phenom. **117**, 41 (2001).

²O. Gunnarsson and K. Schönhammer, Phys. Rev. B **22**, 3710 (1980).

³M. Cini, Solid State Commun. **24**, 681 (1977).

⁴G. A. Sawatzky, Phys. Rev. Lett. **39**, 504 (1977).

⁵P. A. Bennett, J. C. Fuggle, F. U. Hillebrecht, A. Lenselink, and G. A. Sawatzky, Phys. Rev. B **27**, 2194 (1983).

⁶R. W. Lof, M. A. van Veenendaal, B. Koopmans, H. T. Jonkman, and G. A. Sawatzky, Phys. Rev. Lett. **68**, 3924 (1992).

⁷K. Maiti, D. D. Sarma, T. Mizokawa, and A. Fujimori, Phys. Rev. B **57**, 1572 (1998).

⁸V. I. Anisimov, F. Aryasetiawan, and A. I. Lichtenstein, J. Phys.: Condens. Matter **9**, 767 (1997).

⁹G. Seibold, J. Lorenzana, and F. Becca, Phys. Rev. Lett. **100**, 016405 (2008).

¹⁰F. D. M. Haldane, J. Phys. C **14**, 2585 (1981).

¹¹H. J. Schulz, J. Phys. C **16**, 6769 (1983).

¹²T. Giamarchi and H. J. Schulz, Phys. Rev. B **39**, 4620 (1989).

¹³K. Schönhammer and V. Meden, Phys. Rev. B **47**, 16205 (1993).

¹⁴J. Voit, Rep. Prog. Phys. **58**, 977 (1995).

¹⁵V. Meden, Phys. Rev. B **60**, 4571 (1999).

¹⁶J. González, M. A. Martín-Delgado, G. Sierra, and M. A. H. Vozmediano, *Quantum Electron Liquids and High- T_c Superconductivity* (Springer-Verlag, Berlin, 1995), Chap. 4.

¹⁷A. Luther and I. Peschel, Phys. Rev. B **9**, 2911 (1974).

¹⁸J. Voit, J. Phys.: Condens. Matter **5**, 8305 (1993).

¹⁹K. D. Schotte and U. Schotte, Phys. Rev. **182**, 479 (1969).

²⁰K. D. Schotte and U. Schotte, Phys. Rev. **185**, 509 (1969).

²¹O. Gunnarsson and K. Schönhammer, Surf. Sci. **89**, 575 (1979).

²²V. Drchal and M. Cini, J. Phys.: Condens. Matter **6**, 8549 (1994).

²³A. P. Dementjev, K. I. Maslakov, and A. V. Naumkin, Appl. Surf. Sci. **245**, 128 (2005).

²⁴E. Perfetto, M. Cini, S. Ugenti, P. Castrucci, M. Scarselli, M. De Crescenzi, F. Rosei, and M. A. El Khakani, Phys. Rev. B **76**, 233408 (2007).

²⁵B. Gao, A. Komnik, R. Egger, D. C. Glattli, and A. Bachtold, Phys. Rev. Lett. **92**, 216804 (2004).

²⁶Z. Yao, H. W. Ch. Postma, L. Balents, and C. Dekker, Nature (London) **402**, 273 (1999).

²⁷M. Bockrath, D. H. Cobden, J. Lu, A. G. Rinzler, R. E. Smalley, L. Balents, and P. L. McEuen, Nature (London) **397**, 598 (1999).

²⁸R. Egger and A. O. Gogolin, Phys. Rev. Lett. **79**, 5082 (1997); Eur. Phys. J. B **3**, 281 (1998).

²⁹C. Kane, L. Balents, and M. P. A. Fisher, Phys. Rev. Lett. **79**, 5086 (1997).

- ³⁰J. E. Houston, J. W. Rogers, R. R. Rye, F. L. Hutson, and D. E. Ramaker, *Phys. Rev. B* **34**, 1215 (1986).
- ³¹In Eq. (17), we use $G_0^{2D}(-\omega+i0^+)$ instead of $G_0^{2D}(\omega+i0^+)$ because CS theory is formulated in terms of binding energy, while in the present paper, we use the kinetic energy scale.
- ³²A. Goldoni, R. Larciprete, L. Gregoratti, B. Kaulich, M. Kiskinova, Y. Zhang, H. Dai, L. Sangaletti, and F. Parmigiani, *Appl. Phys. Lett.* **80**, 2165 (2002).
- ³³ $\kappa \approx 2$ is the dielectric constant of carbon nanotubes; see, e.g., Ref. 28.
- ³⁴S. Bellucci, J. González, and P. Onorato, *Phys. Rev. Lett.* **95**, 186403 (2005).
- ³⁵In order to compare the low-energy part of Fig. 2 with the experiment reported in Ref. 24, one has to shift the energy scale ω of 284.6 eV, which is the $1s$ core-hole binding energy in the two carbon structures.